Robust NMPC for an Automotive HVAC System AuE8930 Term Project

Mayuresh Bhosale, *AuE,* Maximilian Frantz, *ME,* and Kiran Ganesh, *AuE*

***Abstract*—The increased usage of hybrid and battery electric vehicles has prompted study of methods for optimizing energy consumption of cabin thermal management systems.**

***Index Terms*—MPC, Robust MPC, Hybrid Vehicle, Thermal Management.**

I. Nomenclature

$T_{ea} = Evaporator\ air\ temperature\ (K)$
$T_{eaR} = Reference\ evaporator\ air\ temperature\ (K)$
$\dot{m} = Evaporator\ fan\ mass\ flow\ rate\ (kg/s)$
$T_b = Vehicle\ body\ temperature\ (K)$
$T_c = Cabin\ air\ temperature\ (K)$
$c_{pa} = Specific\ heat\ capacity\ of\ cabin\ air\ (J/(kg * K))$
$\rho_c = Air\ density\ in\ cabin\ (kg/m^3)$
$V_c = Cabin\ air\ volume\ (m^3)$
$c_{pea} = Specific\ heat\ of\ evaporator\ air\ (J/(kg * K))$
$\dot{Q}_{met} = Passenger\ metabolic\ load\ (W)$
$C_b = Body\ thermal\ capacity(J/K)$
$\dot{Q}_{sol} = Solar\ radiation\ load\ (W)$
$\dot{Q}_{ab} = Body\ and\ ambient\ air\ convection\ (W)$
$v_{veh} = Vehicle\ velocity\ (m/s)$
$C_c = Cabin\ air\ thermal\ capacity\ (J/K)$
$A_{ab} = Outer\ body\ area\ (m^2)$
$A_{fan} = Evaporator\ fan\ area\ (m^2)$
$A_{cb} = Inner\ body\ area\ (m^2)$

II. Introduction

AS control technology becomes more sophisticated; it opens up opportunities in the automotive industry to improve overall vehicle efficiency—whatever the powertrain architecture may be (combustion engine, electric vehicle or hybrid)—by more efficiently controlling various vehicle systems. One example where a lot of energy is used in any vehicle at any given time is the heating or cooling of the occupant cabin. In conventional ICE vehicles, the A/C compressor is run by the engine but as the industry moves towards EVs, the constant high load on the battery powering the HVAC systems causes a lot of energy usage and can be optimized to achieve better vehicle efficiency and hence reduce range anxiety.

Lately, a lot of vehicle cabin thermal management work has focused on controlling energy usage of the cabin HVAC system via Model Predictive Control (MPC). Since the physical plant model (A/C + cabin) is a complicated nonlinear system, many approaches done so far start with a simple linearized model without environmental thermal disturbances to the cabin from solar and convective energy.

While establishing the controller, there are various approaches taken in terms of choosing the states, control inputs, measured outputs and external disturbances. The work in [1] focuses on optimal set point tracking of the heat power request from the passenger and the state of charge of the battery in a hybrid vehicle, making use of additional energy requests to the ICE motor to supplement the heat from conventional HVAC components. In [2], the authors implement Adaptive MPC on real BEV hardware to optimize set point tracking of cabin air temperature. To account for the disturbances lacking in these works, the work of others, such as the authors of [3] is invaluable for accurate disturbance estimation, where a complete thermal model of a vehicle cabin is made accounting for heat transfer through all the vehicle body surfaces like the roof, windows, windshield etc.

Others have accounted for such disturbances in the system. In [4], external factors to the system, like vehicle velocity, ambient temperature and solar radiation, are taken into account as disturbances. One more potential disturbance is the metabolic rate of the cabin occupant, as in [5]. When propulsion is integrated into the thermal management model, there are more variables and disturbances like road slope [7].

In addition to the MPC formulation for the tracking of set cabin temperature, some works have accounted for the thermal comfort of the occupant through the Predicted Mean Vote (PMV) method [4], [5]. PMV depends on six factors – air temperature, air velocity, mean radiant temperature, air relative humidity, clothing insulation, and metabolic rate [12]. These can be assumed, like in [5] or calculated as in [4], and the output of the PMV function attempts to characterize a representation of how hot or cold the occupant feels at any given moment. This comfort component is also added to the objective function formulation.

Furthermore, the model in [4] also includes an "intelligent" section that uses a Back Propagation Neural Network (BPNN) that is trained to run a Vehicle Speed Previewer (VSP). This attempts to predict the future vehicle speed for a prediction horizon of 100 s, which helps in understanding the loads that the HVAC system might potentially go through in the upcoming few moments. Since the operation of the HVAC system majorly affects the usable energy of an EV, it is inferred that more research must be done to come up with a robust controller that optimizes this system so as to maximize energy savings and improve overall vehicle efficiency.

With the rise of autonomous vehicles, the human experience inside the cabin plays a bigger role than in conventional vehicles. Hence, an algorithm to incorporate the thermal comfort of the occupants within the HVAC controller is a crucial

element in an autonomous vehicle system. In this project, we plan to achieve a robust control algorithm for the cabin temperature management of an electric vehicle using MPC and also consider the thermal comfort of the occupant using a PMV model.

III. Model

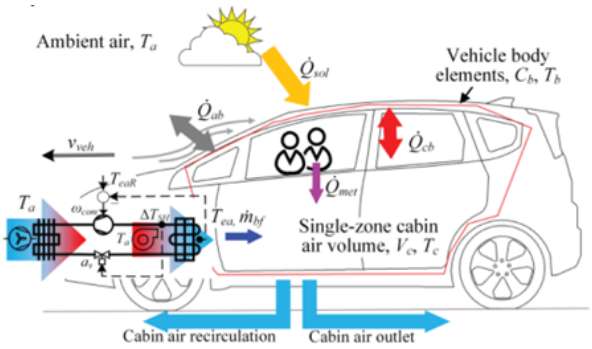

Fig. 1: Illustration of single zone passenger cabin model [5]

A. Control-oriented model of AC and Cabin coupled system

The problem in section 1 has been addressed by proposing a robust cabin climate management system. External disturbances such as heat through windows, windshield and the vehicle body are considered in this approach. Figure 1 represents the overall schematic of the system that affects the temperature dynamics. This section represents the dynamic model of HVAC and the cabin coupled thermal system to control the cabin thermal comfort index. The HVAC system comprises the following components: the compressor, condenser, expansion valve, and evaporator, all of whose dynamics are well understood [8]. The Cabin system comprises the mass air flow from the HVAC blower and temperature evolution based on the heat flow between the vehicle and the external environment. For the compressor, the refrigerant mass flow rate is calculated based on the volumetric efficiency and isentropic efficiency at different speeds. The modeled flow coefficient is taken from [5] for the expansion valve to give the mass flow rate of refrigerant R134a. Heat transfer coefficients for the evaporator and condenser are also obtained from [5].

1) HVAC modeling: HVAC systems are often modeled with a 12th order differential equation. However, work has been done to show that this system can be accurately approximated by a system of 2nd order differential equations as in [5], [6]. The resulting 2nd ODE a function of the evaporator air temperature dynamics (T_{ea}), it's setpoint (T_{eaR}) and the evaporator fan mass flow rate ($\dot{m}$) is given by equation 1 below.

$$\ddot{T}_{ea}\tau_w^2(\dot{m}) + 2\zeta\tau_w(\dot{m})\dot{T}_{ea} + T_{ea} = \tau_z(\dot{m})\dot{T}_{ea} + T_{eaR} \quad (1)$$

The 2nd order model for the HVAC requires determining time constants and a damping parameter. Due to the inability to determine real parameter values for the HVAC system via experimentation, parameters were taken from from [5]. The damping coefficient was recommended to be 0.7 and experimental values for the time constants as a function of mass flow rate of the fan were read from a plot and fit with a cubic polynomial (Figure 3). After this fit was established, the time constants were scheduled with respect to u_2 in state space equations 7 and 8. The 2nd order HVAC model saw simulated and found to behave as expected based on [5].

2) Cabin modeling: The thermodynamics of air in a vehicle cabin interacting with the HVAC and external environment is discussed in [3]. The differential equations that drive the dynamics are given in equations 2-3. These equations describe the vehicle body temperature (T_b) and cabin air temperature (T_c) evolution with respect to each other, the HVAC system, and environmental factors.

$$c_{pa}\rho_c V_c\dot{T}_c = \dot{m}c_{pea}(T_{ea} - T_c) + \dot{Q}_{met} + k_{cb}(T_b - Tc) \quad (2)$$

$$C_b\dot{T}_b = -k_{cb}(Tb - T_c) + \dot{Q}_{sol} + \dot{Q}_{ab} \quad (3)$$

where

$$\dot{Q}_{ab} = (4.65 + 13.95\sqrt{v_{veh}})A(T_a - Tb) \quad (4)$$

describes the convection between the external air and the vehicle body.

Cabin temperature T_c and fan $\dot{m}$ are the two variables that most affect passenger comfort. As in the state space equations below, heat transfer and thermodynamic parameters were obtained from [3], [8], [10].

B. Coupled State Space model

In state space, these equations are given by $\dot{x}_1$ and $\dot{x}_2$ below, where $C_c = c_{pa}\rho_c V_c$ is the heat capacity of the cabin air, respectively, A_{ab} and A_{cb} are the internal and external body surface areas, A_{fan} is the total outlet area of the A/C vents, and c_{ea} and ρ_{ea} are the evaporator-side air specific heat and density, respectively. Sources for these parameters are the same as above.

The evolution of the two HVAC states is expressed in $\dot{x}_3$ and $\dot{x}_4$ below, where the physical state of interest is the evaporator outlet temperature. The purpose of u_1–the requested temperature of the air coming out of the vent–is to simulate the actual time required for the HVAC system to change the temperature of the ambient external air to the requested air temperature.

The state space equations are given by:

$$\dot{x}_1 = -\frac{2.8A_{cb}}{C_c}x_1 + \frac{2.8A_{cb}}{C_c}x_2 - \left(\frac{c_{pea}}{C_c} + \frac{3A_{cb}}{C_cA_{fan}\rho_{ea}}\right)x_1u_2 + \frac{3A_{cb}}{C_cA_{fan}\rho_{ea}}x_2u_2 + \frac{c_{pea}}{C_c}x_3u_2 + \frac{1}{C_c}d_4 \quad (5)$$

$$\dot{x}_2 = \frac{2.8A_{cb}}{C_b}x_1 - \frac{2.8A_{cb} + 4.65A_{ab}}{C_b}x_2 + \frac{3A_{cb}}{C_bA_{fan}\rho_{ea}}x_1u_2 - \frac{3A_{cb}}{C_bA_{fan}\rho_{ea}}x_2u_2 - \frac{13.95A_{ab}}{C_b}x_2\sqrt{d_2} + \frac{4.65A_{ab}}{C_b}d_1 + \frac{13.95A_{ab}}{C_b}d_1\sqrt{d_2} + \frac{1}{C_b}d_3 \quad (6)$$

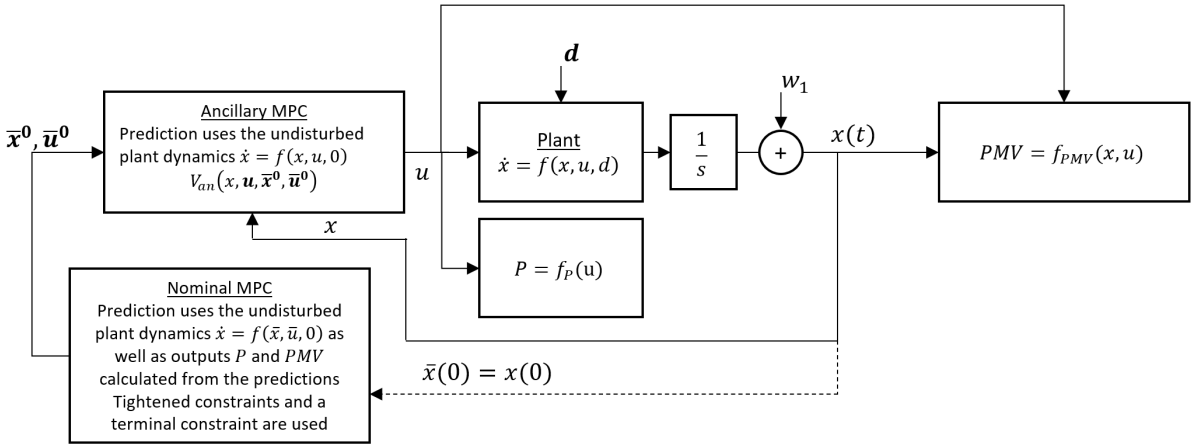

Fig. 2: MPC flowchart

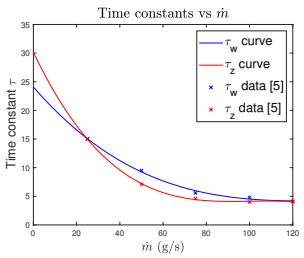

Fig. 3: HVAC time constants as a function of $\dot{m}$

$$\dot{x}_3 = x_4 + \frac{\tau_z(u_2)}{\tau_w^2(u_2)} u_1 \tag{7}$$

$$\dot{x}_4 = -\frac{1}{\tau_w^2(u_2)} x_3 - \frac{2\zeta}{\tau_w(u_2)} x_4 + \frac{\tau_w(u_2) - 2\zeta\tau_z(u_2)}{\tau_w^3(u_2)} u_1 \tag{8}$$

States: $\mathbf{x} = [T_c, T_b, T_{ea}, \dot{T}_{ea} - \frac{\tau_z(\dot{m})}{\tau_w^2(\dot{m})} T_{eaR}]^T$, where T_c, T_b and T_{ea} the the cabin air, body and evaporator air temperatures and x_4 is not a physically meaningful state. It is assumed x_1, x_2, x_3, an observer is used for x_4.

Inputs: $\mathbf{u} = [T_{eaR}, \dot{m}]^T$, where T_{eaR} is the cabin inlet air temperature reference and $\dot{m}$ is the mass flow rate of air from the vents.

Disturbances: $\mathbf{d} = [T_a, v_{veh}, \dot{Q}_{sol}, \dot{Q}_{met}]^T$, where T_a is the ambient air temperature, v_{veh} is the vehicle speed, $\dot{Q}_{sol}$ is the solar heat, and $\dot{Q}_{met}$ is the passenger metabolic heat. It is assumed that d_1 and d_2 are known from vehicle instrumentation. The disturbances that are uncertain are the two heats, but they are bounded and the controller can be made robust against them, as demonstrated below.

C. Model Predictive Control

A tube-based approach to robust NMPC was used. 2 shows the overall flowchart of the cabin climate control system. The Tube-based NMPC approach was referred from Rawlings [13]. The plant (Eqs. 5-8) is subject disturbance. The initial current state is first fed into the Nominal MPC, which generates an optimal control sequence and trajectory for the nominal (undisturbed) system. An ancillary MPC then generates the optimal control action for the disturbed system. The goal of this formulation is to attain the required set temperature demanded by the passenger, maximize the passenger comfort (PMV) and minimize overall power consumed by the system while preventing the evaporator wall from frosting. PMV was calculated from the set of equations provided in [12]. The equation for power was obtained from [5] and takes into account the power consumption by the compressor and the evaporator fan via u_1 and u_2, respectively, as these are the two predominant sources of power consumption in the HVAC system.

1) Nominal MPC: With the above goal in mind, the cost function $\bar{V}_N$ for the nominal MPC was selected as follows, with $\bar{x}(i=0) = x(t)$:

$$\bar{V}_N(\bar{x}, \bar{\mathbf{u}}) = \sum_{i=0}^{N-1} [q(x_{1R} - \bar{x}_1(i))^2 + p\bar{P}(i)^2 + m\overline{PMV}(i)^2 + s_1\Delta u_1(i)^2 + s_2\Delta u_2(i)^2]$$

where

$$\overline{PMV} = f_{PMV}(\bar{x}_1, \bar{u}_2, RH, met, clo, wme) \text{ and}$$
$$\bar{P} = f_P(\bar{u}_1, \bar{u}_2)$$

The weights used in $\bar{V}_N$ were $q = 10, p = 5, s = 0.3$, and $m = 0.1$. The other parameters for PMV were relative humidity $RH = 15\%$, and metatbolic rate $met = 1.1$, clothing factor $clo = 1$ for a warm day and external work $wme = 0$, all suggested by [12]. The Nominal MPC then solved the following optimization problem to attain the optimal nominal control sequence and trajectory:

$$\min_{\mathbf{u}} \bar{V}_N(\bar{x}, \bar{\mathbf{u}}) \text{subject to}$$
$$\dot{\bar{x}} = f(\bar{x}, \bar{u}, 0)$$
$$\bar{x} \in \bar{\mathbb{X}}, \bar{u} \in \bar{\mathbb{U}}$$
$$\bar{x_N} = x_{1R}, \text{ where}$$
$$\bar{\mathbb{X}} = \{x \in \mathbb{R}^4 | x_3 > 278\} \quad \text{and}$$
$$\bar{\mathbb{U}} = \{u \in \mathbb{R}^2 | u_1 > 280, 0.033 < u_2 < 0.088\}$$

Time did not permit the use of Monte Carlo simulation to determine the loosest constraints to use with the Nominal MPC. See the Conclusion for more discussion of how this would have been done, time permitting.

2) Ancillary MPC: The ancillary controller chosen for this system is a secondary MPC. To drive the system towards the nominal trajectory, the cost function V_{an} was selected as follows:

$$V_{\text{an}}(x, \mathbf{u}, \bar{\mathbf{x}}^0, \bar{\mathbf{u}}^0) = \sum_{i=0}^{N-1} [|x(i) - \bar{x}^0(i)|_Q^2 + |u(i) - \bar{u}^0(i)|_R^2 + |\Delta u(i)|_S^2] + V_f(x(N))$$

where $\bar{\mathbf{x}}^0$ and $\bar{\mathbf{u}}^0$ are the optimal nominal state sequence and input sequence determined by the nominal MPC. The weights used were $Q = 10I$ and $R = S = I$.

The ancillary MPC then solved the following optimization problem to attain the optimal control action to apply to the plant:

$$\min_{\mathbf{u}} V_{an}(x, \mathbf{u}, \bar{\mathbf{x}}^0, \bar{\mathbf{u}}^0) \text{subject to}$$
$$\dot{x} = f(x, u, 0)$$
$$u \in \mathbb{U}, \text{ where}$$
$$\mathbb{U} = \{u \in \mathbb{R}^2 | u_1 > 280, 0.005 < u_2 < 0.09\}$$

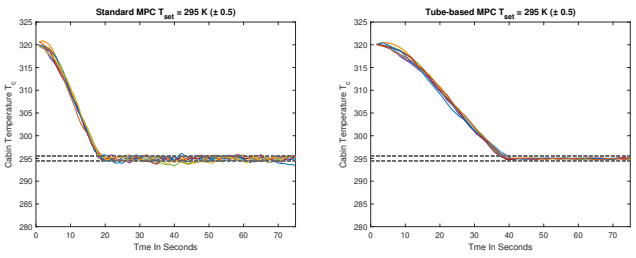

Fig. 4: Reference temperature 295 K with disturbance bounds [-0.5 0.5]

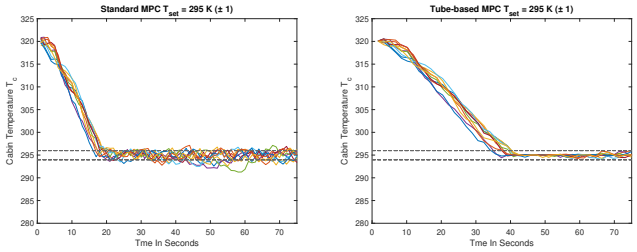

Fig. 5: Reference temperature 295 K with disturbance bounds [-1 1]

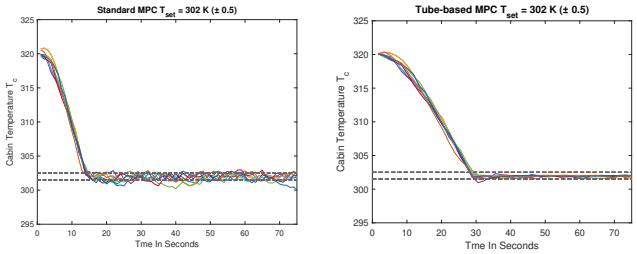

Fig. 6: Reference temperature 302 K with disturbance bounds [-0.5 0.5]

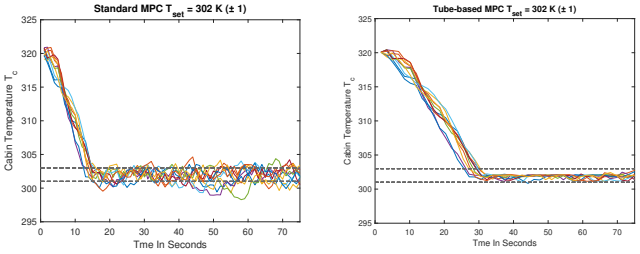

Fig. 7: Reference temperature 302 K with disturbance bounds [-1 1]

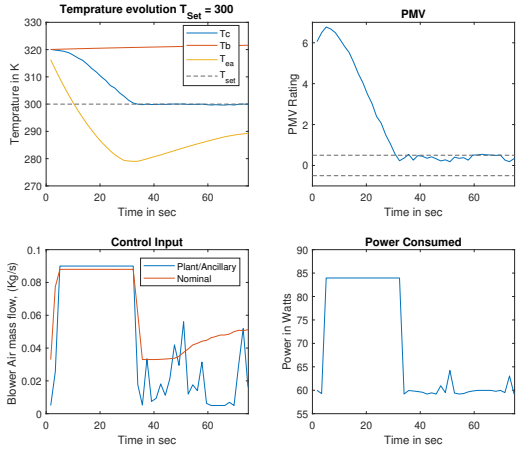

Fig. 8: Tube-based NMPC

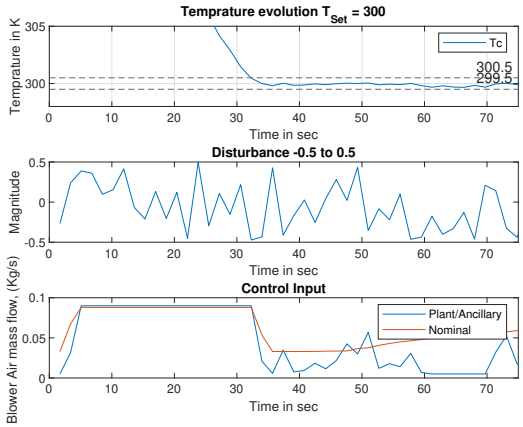

Fig. 9: Tube-based NMPC disturbance

to satisfy the constraints on T_c, but at the cost of taking additional time to reach the target. However, as shown in Figure 10, the faster decrease in temperature comes with a power consumption penalty. If the goal is to save energy, this may not be desired.

Figures 6 and 7 show that the standard MPC has even more trouble staying within the constraints if the starting temperature is further from the setpoint temperature. By comparison, the robust controller is capable of maintaining the constraints.

The state evolution for the three physically meaningful states, the PMV and the Power consumption, is shown in Figure 8. This figure also shows the difference between the nominal control sequence for the fan mass flow rate vs. the actual control sequence applied by the ancillary MPC. The tighter constraint on the nominal control can be observed here.

A typical disturbance sequence with $w_1 \in [-0.5\ 0.5]$ is shown in Figure 9.

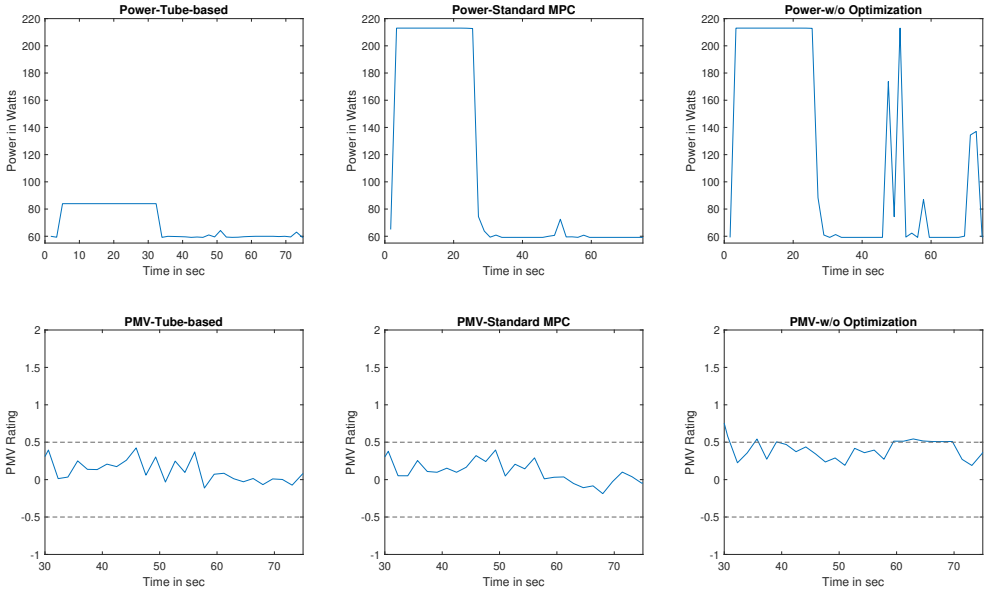

Fig. 10: Power and PMV figures

IV. Simulations and Results

Simulations were run using a time step of 1.7 seconds and simulated for 130 seconds. A 30-step horizon length was used for both MPCs.

For disturbance vector $\mathbf{d}$, $T_a = 320$ K and $v_{veh} = 11$ m/s were kept constant through the simulations. The values for $\dot{Q}_{sol}$ and $\dot{Q}_{met}$ where likewise kept constant. However, a random disturbance w_1 of a given band was added to the cabin temperature x_1 at the beginning of the feedback loop. This disturbance represents uncertainty in the actual disturbance vector $\mathbf{d}$ and its effect on the cabin temperature. Different bands of disturbance were simulated for several sequences of the given disturbance band. Two different values of T_{cR}, $295K$ and $302K$ were also explored.

Figures 4 and 5 compare a standard MPC to the tube-based robust MPC. In both cases, the robust controller is able

V. Conclusion and Further Research

This paper demonstrates the differences between a tube-based robust NMPC system and a standard MPC for controlling cabin temperature in a vehicle subject to environmental disturbances. The tube-based controller was able to maintain a temperature setpoint within tight constraints, where the standard MPC violated these. The standard MPC drove the cabin temperature to the setpoint faster but at the cost of using more power and leaving the desired bounds for cabin temperature at a steady state.

One aspect that should be pursued in the future is a comparison of power consumption for long periods of steady-state operation. Based on the results shown in this paper, it is predicted that the tube-based controller would outperform the standard MPC with respect to long-term steady-state power consumption, but confirming this would add evidence to the case for using the robust controller in real-world applications. Additionally, simulating over a realistic drive cycle, such as one where doors open to let ambient air in, passengers get in and out of the car, etc., would be good to demonstrate the robust controller's ability to handle these situations better than a standard controller.

As with all nonlinear MPC problems, much work could be done to improve computation time before the tube-based controller could be applied in a vehicle. The typical runtime for one iteration of the loop was 0.8 seconds. This could be reduced by simplifying certain computations, for instance, by creating a lookup table or lower-order fit for the PMV calculation.

Finally, as mentioned above, time limitations prevented a thorough exploration of constraint tightening via Monte Carlo simulation. Given time, the authors would perform a search for the loosest constraints $\bar{\mathbb{X}}, \bar{\mathbb{U}}$ that would guarantee with high confidence that constraints would not be violated over the life of the vehicle.

Acknowledgment

The authors would like to thank Professor Ayalew for teaching and thoroughly challenging us.

References

[1] H. Esen, T. Tashiro, D. Bernardini and A. Bemporad, *Cabin Heat Thermal Management in Hybrid Vehicles using Model Predictive Control*, IEEE 22nd Med. Conf. on Cont. and Aut., June 2014.

[2] P. Fussey, H. Ma and N. Dutta, *Application of Model Predictive Control to Cabin Climate Control Leading to Increased Electric Vehicle Range* SAE Technical Paper 2023-01-0137.

[3] D. Marcos, F. J. Pino, C. Bordons and J.J. Guerra, *The development and validation of a thermal model for the cabin of a vehicle*, Applied Therm. Eng., vol. 66, pp. 646-656, 2014.

[4] Xie, Y., Liu, Z., Li, K., Liu, J., Zhang, Y., Dan, D., Wu, C., Wang, P., and Wang, X. (2021), *An improved intelligent model predictive controller for cooling system of electric vehicle*, Applied Thermal Engineering.

[5] I. Cvok and J. Deur, *Nonlinear model predictive control of electric vehicle cabin cooling system for improved thermal comfort and efficiency*, 2022 European Control Conference (ECC), 2022.

[6] I. Ratkovic, I. Cvok, V. Soldo, J. Deur, *Control-oriented Modelling of Vapour-Compression Cycle Including Model-order Reduction and Analysis Tools*, Conference Paper, October 2019.

[7] F. Ju, N. Murgovski, W. Zhuang, and L. Wang, *Integrated propulsion and cabin-cooling management for Electric Vehicles* Actuators, vol. 11, no. 12, p. 356, 2022.

[8] Y. Huang, A. Khajepour, F. Bagheri and M. Bahrami, *Optimal energy-efficient predictive controllers in automotive airconditioning/refrigeration systems*, Applied Energy, vol. 184, pp. 605-618, 2016.

[9] X.D. He, H.H. Asada, S. Liu and H. Itoh, *Multivariable Control of Vapor Compression Systems*, HVAC&R Research, vol. 4, no. 3 July 1998.

[10] S.Y. Yoo and D.W. Lee, *An Experimental Study on the Performance of Automotive Condenser and Evaporator*, Int. R and AC Conf., 2004.

[11] J. Wu, F. Jiang, H. Song, C. Liu and B. Lu, *Analysis and validation of transient thermal model for automobile cabin*, Applied Thermal Eng., vol. 122, pp. 91-102.

[12] *Thermal Environmental Conditions for Human Occupancy*, ASHRAE Standard 55-2020

[13] *J B. Rawlings,D Q. Mayne, Diehl, Book - Model Predictive Control, Theory, Computation, and Design*, Second Edition